Light-induced Properties of Doped $Bi_4Ge_3O_{12}$ Single Crystals

Vera Marinova[a], Shiuan H. Lin [b], Marin Gospodinov [c], Ken. Y. Hsu[a]
[a] Institute of Electro-Optical Engineering, National Chiao Tung University, HsinChu 30050, Taiwan
[b] Department of Electrophysics National Chiao Tung University, HsinChu 30050, Taiwan
[c] Institute of Solid State Physics, Bulgarian Academy of Sciences, 1784 Sofia, Bulgaria

ABSTRACT

Optically homogeneous bismuth germanate $Bi_4Ge_3O_{12}$ single crystals doped with vanadium, cobalt and vanadium plus cobalt have been successfully grown by Czohralski technique with automatically diameter-weight control. The distribution coefficients for individual doping elements are determined. The effect of doping on the light-induced properties of BGO single crystals is studied. Optical absorption spectrum of annealed samples can be strongly modified under ultraviolet illumination. The photochromic effect is optically or thermally reversible from one state to another. Volt-amper charactersitcs show linear behavour and dark conductivity values are $\sigma \sim 10^{-13}$ $(\Omega.cm)^{-1}$. Holographic grating were successfully recorded in all investigated doped crystals at 514 nm.

Keywords: doped crystals, optical properties, photochromic effect, photorefractive effect,

1. INTRODUCTION

Germanium oxide $Bi_4Ge_3O_{12}$ (BGO) crystals crystallize in *43m* point group symmetry with a cubic structure (known as eulytite) and does not exhibit natural liner birefringence. BGO crystals have large transparency range starting from 280 nm to approximately 6 μm and they are not optically active [1]. Optical, thermo-optic, electro-optic and photoelastic properties have been studied on non-doped BGO [2].

BGO crystals are attractive materials for scintillating applications as x-ray, γ-ray and positron detectors because of their room-temperature luminescence [3].

Recently, BGO shows another interesting properties - photorefractive effect. Similar to $LiNbO_3$, undoped BGO is one of the few crystals showing photorefractivity in the ultraviolet spectrum spectrum at room temperature [4,5]. For the first time photorefractive properties of BGO at UV region were reported by Montemezanni et al in 1994 [5]. However, in undoped BGO there is not enough density of suitable traps for the photoinduced charge carriers and it is not possible to modulate the refractive index in the visible spectral range. In order to improve the photorefractive sensitivity, appropriate dopants can be added in a wide gap BGO structure, which appears to be a suitable matrix for extrinsic impurities. For the first time holographic gratings at 442 nm were recorded in BGO crystals doped with Cr [6]. Recently, photorefractive effect in visible spectral range has been observed in BGO doped with iron, manganese, cobalt and chromium [7,8]. The presence of point defects or doping ions in the crystal structure leads to generation of a charge transfer process responsible for photorefractive effect. Inhomogeneous laser illumination created by the interference of the reference and signal beam excites charge carriers from impurity levels into the conduction or valence bands, the charge carriers migrate (by diffusion or drift) and finally are trapped by empty impurities. The resulting space charge field modulates the refractive index via the electro-optic effect.

Together with photorefractive phenomena, photochromic effect was observed in all doped BGO crystals, mentioned above [7,9]. Such simultaneously existence of photorefractive and photochromic effects open a new possibility to use doped BGO crystals for two-center recording, recently proposed by Buse at el. [10] as a solution of the problem of volatility in holographic read–write memory. For this purpose detailed investigations of different dopants influence on the optical and holographic properties in BGO structure is necessary in order to improve the crystal performance in desired direction.

In this paper, we report the influence of V, Co and V+Co doping on light-induced properties. For the first time dark conductivity data are reported.

Proceedings of SPIE Vol. 5206 Photorefractive Fiber and Crystal Devices: Materials, Optical Properties, and Applications IX, edited by Francis T. S. Yu, Ruyan Guo, Shizhuo Yin (SPIE, Bellingham, WA, 2003) · 0277-786X/03/$15.00

2. EXPERIMENT

2.1. Crystal growth

BGO single crystals doped with vanadium, cobalt and co-doped were obtained by Czochralski technique. A stoihiometric Bi_2O_3:GeO_2 powders were mixed in molar proportion 2:3. Growing was performed from melts in pure platinum crucibles of diameter 100 mm and 120 mm high. The crucible weighting method for crystal diameter control was applied. The growth conditions for BGO crystals have been established by adjusting the temperature gradient above the melt and the optimal conditions are summarized in Table 1.

Table 1. Optimal conditions for growing process of BGO crystals

Crucible	pure platinum, high 120 mm, diameter 100 mm
Heater	Crucilite heating element, 3 kW
Pull rate	0.08-0.3 mm/h
Crystal rotation rate	20 to 40 rot/min
Pulling direction	[001], [110], [111]
Temperature gradient above the melt	ca. 50-70°C cm^{-1}
Annealing condition	24h at 750°C
Cooling rate	20°C/hour from 750°C to room temperature

Vanadium and cobalt were introduced into the melt in form of oxides - V_2O_5 and Co_3O_4. Distribution coefficient κ for individual doping elements was calculated as the ratio between molar concentrations of dopants into the crystal to the molar concentration of the same elements into the melt.
The doping elements content was determined by flame and electro-thermal atomic absorption spectrometry (ETAAS). The doped crystals compositions and the obtained values for distribution coefficient are summarized in Table 2.

Table 2. Dopands concentration and distribution coefficient

Dopand	V	Co	V+Co
Concentration (cm^{-3})	6.8×10^{18}	1.1×10^{18}	V - 4.8×10^{18} Co - 4.6×10^{18}
Distribution coefficient ***k***	0.2	0.08	

For optical measurements double polished crystal plates with 20 mm in diameter and 1 mm thickness were prepared.

2.2. Absorption and light-induced absorption

Optical transmission spectra were measured on crystal plates in the wavelength range 280-1500nm using Cary 5I model spectrophotometer. Reflection spectra were measured on plates with one polished and one grinded side in 300-800nm wavelengths interval using Perkin-Elmer 330 spectrophotometer with special references for calibrations at 488; 514.5; 576; 633 and 672 nm. The absorption coefficient $\alpha(cm^{-1})$ was calculated using the formula:

$$T = \frac{(1-R^2)\exp(-\alpha d)}{1+R^2\exp(-2\alpha d)} \qquad (1)$$

where: T stands for the transmission coefficient, R - for the reflection coefficient and d for the plate thickness.
The light-induced absorption changes were measured on two different initial states of the crystals:
(i) annealed state - after heating in oven at 400°C for 2 hours. The thermal annealing leads to a maximum value of transmission and we consider this state as "bleached" state. During the annealing, the crystal temperature was measured by calibrated platinum thermo-couple fixed on the sample.
(ii) colored state - after preliminary illumination with ultraviolet light coming from Xe lamp source (300 W). UV illumination durations were around 80-100 min in order to obtain the saturation value of the coloration effect. We called the saturated state "coloration" state.

2.3. Dark conductivity

The dark-conductivity measurements were carried out using Keithley 6487 Pico-Ammeter /Voltage Supply. Silver surface electrodes separated by 0.2 ÷ 0.5 mm gap were made.

At the beginning of each experiment the samples were on a “bleached" state. Furthermore, we waited several minutes after any change of voltage supply before the measurement value is taken in order the sample to reach an equilibrium state.

2.4. Holographic recording

Holographic gratings were recorded by two-wave mixing set-up at 514 nm wavelength coming from an Ar^+ laser source. The holographic recording was performed with ordinary polarization of subject I_S and reference I_R interfering beams with intensities 35 mW/cm^2 and 42 mW/cm^2, respectively. Read-out was performed by He-Ne laser probe beam at 633 nm, which enters the crystals at the Bragg angle. The power of the probe beam was 22 mW. Shutter is used to block one of the writing beams during the reading process. The diffracted beam intensity was monitored by a photodetector. Before each holographic experiment the samples were illuminated with UV light for 1 hour.

3. RESULTS AND DISCUSSIONS

3.1. Transmission spectra

The transmission spectrum dependence on wavelength for V, Co and V+Co co -doped BGO crystals is shown in Fig. 1. The instead figure is transmission spectra of undoped BGO for comparison. As it seen in V-doped sample the transmission edge is shifted to the visible spectra (approximately at 380 nm) in comparison with undoped BGO In case of Co-doped the transmission edge is around 325 nm wavelength and a strong transmission peak is located around 570 nm. Furthermore, three absorption bands at 685 nm, 745 nm and 815 nm appeared. Most probably these bands are due to the co-existence of several cobalt oxidation states. In case of cobalt and vanadium as co-doping elements the transmission edge is shifted to the visible range in comparison with single Co- or V-doped and undoped BGO crystals. Strong peak at 580 nm appears, which probably is due to the cobalt contribution. As can be seen from Fig. 1 for co-doped sample, the transmission behaviour until 625 nm is similar to that of as Co-doped crystal, whereas at longer wavelength vanadium has more contribution.

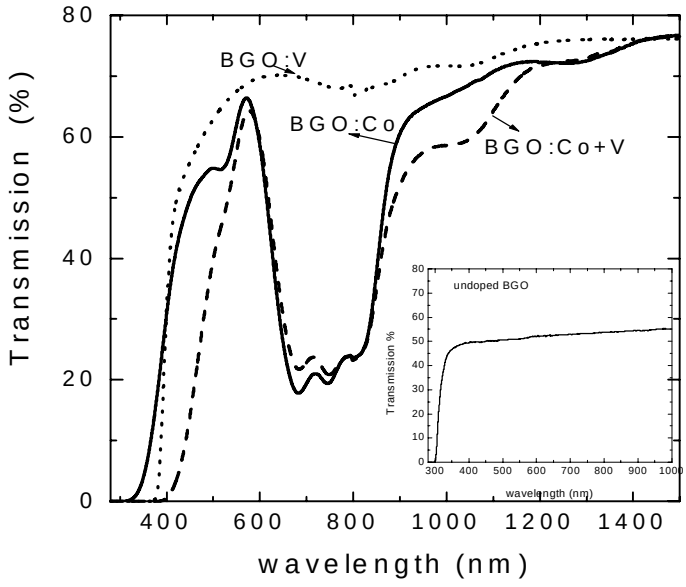

Fig.1. Transmission spectra of BGO crystals doped with V, Co and V+Co. Inset figure–transmission spectrum for undoped BGO.

3.2. Light-induced absorption

Homogeneous illumination with UV light generates light-induced absorption changes in all samples. After illumination the absorption coefficient $\alpha(cm^{-1})$ is changed due to the charge carriers redistribution between different traps. All investigated doped crystals show a significant increase of optical absorption in the colored state. Such increase of the absorption probably is due to the charge transfer transitions of the impurities, which exist simultaneously in samples at different oxidation states.

Light-induced absorption $\Delta\alpha_{ph}$ is calculated using the difference between absorption spectra of the crystal in the colored state and in the bleached state:

$$\Delta\alpha_{ph} = \alpha_{\substack{colored \\ state}} - \alpha_{\substack{bleached \\ state}} \qquad (2)$$

Optical absorption changes versus photon energy in annealed state and after UV illumination maximum are plotted on Fig.2, Fig. 3 and Fig. 4. Additionally, maximum changes of absorption coefficient are shown for each sample. As it seen, the photochromic effect in co-doped samle is stronger than in V and Co-doped samples

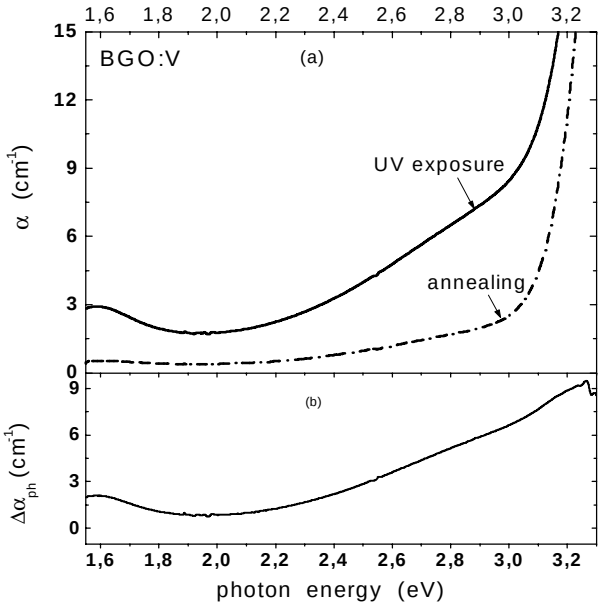

Fig.2. (a) Optical absorption of BGO:V in: (a) annealed state (dash line) and after illumination (straight line) , (b) maximum light-induced absorption changes versus photon energy.

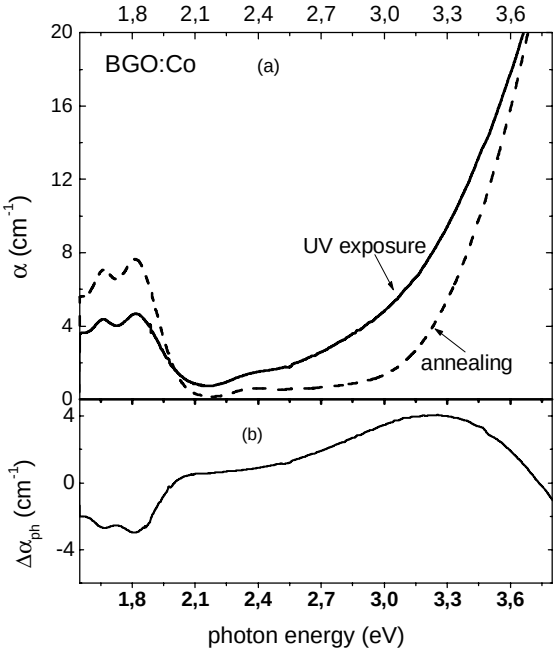

Fig.3. (a) Optical absorption of BGO:Co in annealed state (dash line) and after illumination (straight line) , (b) light-induced absorption (UV-annealing)

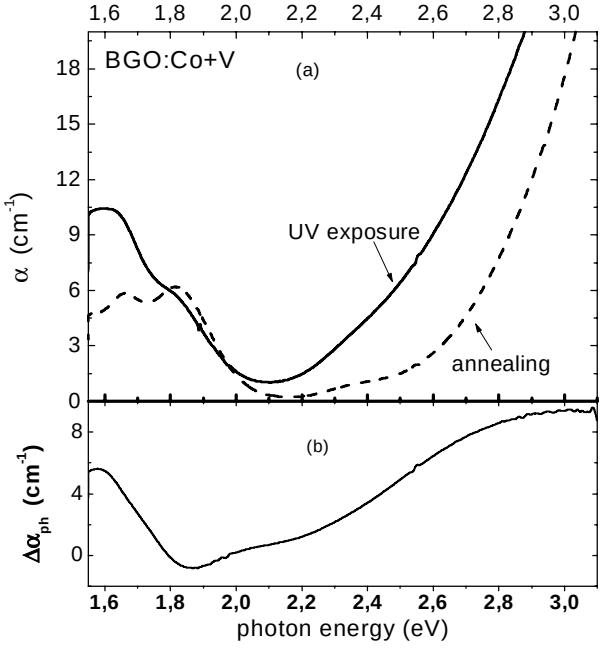

Fig.4. (a) Optical absorption of BGO:V+Co in annealed state (dash line) and after illumination (straight line) , (b) light-induced absorption (UV-annealing)

3.3. Volt-Amper characteristics

Current-voltage characteristics for all investigated crystals in dark conditions at room temperature are shown in Fig. 5. As it seen the measured current-voltage characteristics show linear behavior. The measured dark resistivity at room

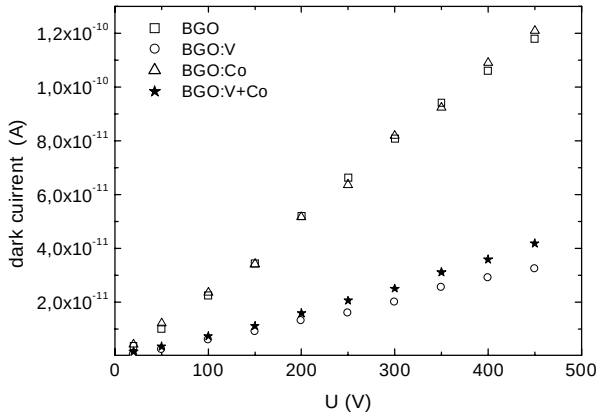

Fig.5. I-V characteristics under dark condition at room temperature

temperature is $\sigma \sim 10^{-13}$ $(\Omega.cm)^{-1}$. These values are similar to data, reported in [5] for undoped BGO.

3.4. Holographic properties

The holographic set-up for two-beam coupling is shown in Fig. 6. The dynamic behaviour of diffracted beam during holographic recording at 514 nm and readout with 633 nm of doped BGO crystals at an incident angle Θ=20° is shown in Figures 7 and 8. The elementary holograms were recorded without external electric field therefore only diffusion mechanism takes part in charge redistribution inside the crystals.

As can be seen from Fig. 7 in case of V-doped BGO crystals, the diffracted signal first increased very fast and after a few second reaches a stationary value. During the reading process, part of the recorded information is still keeping for 3 times longer period than necessary time to reach the saturation state. Obviously, doping with vanadium leads to faster speed during writing in comparison with other doped BGO crystals, where the processes are rather slower and saturation state is reached for several minutes - see Fig. 8. Cobalt doped sample is the slowest one, whereas possess the highest intensity of diffracted beam. Diffraction efficiency of cobalt doped BGO obtained in this work is about $1.7x10^{-5}$ which is lower than obtained in [6], but similar to those in case of Fe-doped BGO [8]. During these preliminary holographic testing we have used limitation on crystal dimensions and no external electric field so it was not possible to obtain absolute values for the diffraction efficiency and to discuss holographic behavior in details.

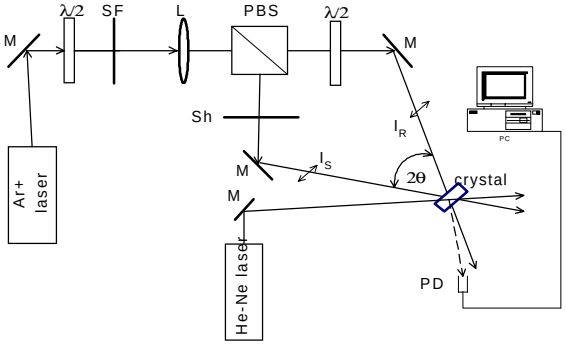

Fig.6. Holographic set-up: M - mirror, L - lens, SF - spatial filter, PBS - polarization beam splitter, PD - photodector, Sh - shutter.

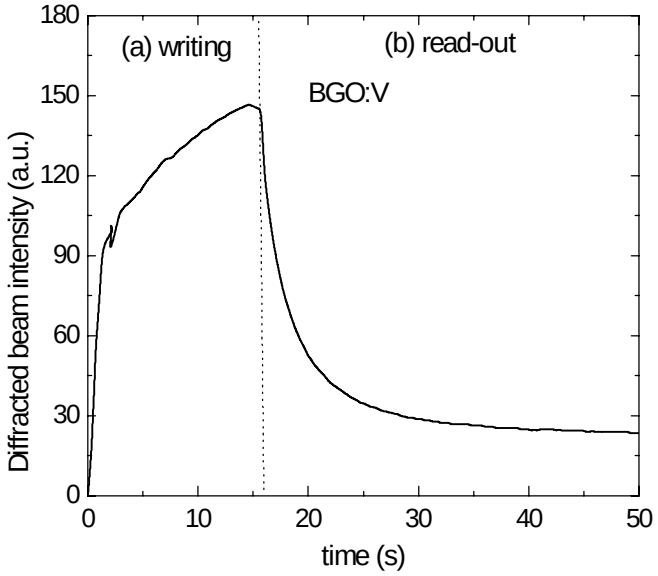

Fig. 7. Dynamics of writing and reading processes during holographic recording in BGO:V. Wavelength of the writing beams is 514nm and probe beam is 633 nm.

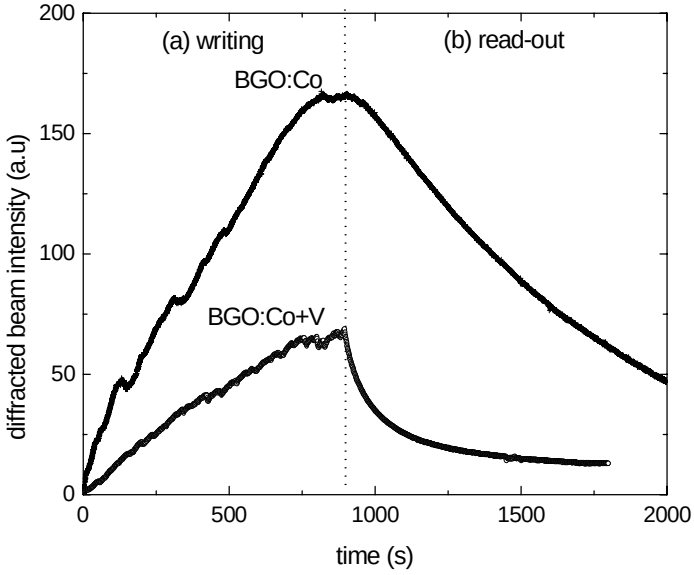

Fig.8. Dynamics of writing and reading processes during holographic recording in BGO:Co and BGO:Co+V. Wavelength of the writing beams is 514nm and probe beam is 633 nm.

It seems that cobalt is the dominant impurity in Co+V doubly doped sample during holographic recording at 514nm, which is confirmed by influence of cobalt on optical properties of Co+V doubly doped sample.

In all investigated doped BGO crystals, due to the enhanced absorption and photochromic effect, photo-induced gratings behavior is rather complex. Probably, the light-induced absorption grating arises because of the presence of shallow traps, which are filled with photoexcited carriers. Since the absorption change magnitude is proportional to the density of filled shallow traps, the shallow-trap grating induced a modulation of the absorption coefficient.

The erasure dynamics in all investigated doped BGO crystals is more complex. Samples need more time to erase the grating than to reach the saturation value during recording. As can be seen from the erasure behavior two different times constants can be determined. The reading processes in Fig. 7 and Fig. 8 show that the formation of absorption grating, originating from UV illumination and inhomogeneous charge population in a shallow trap levels has a much larger erase time constants than the photorefractive one. It could be related that the fast erasure time constant is due to the photorefractive effect and the slower one is due to the photochromic contribution.

CONCLUSIONS

Light-induced absorption of bismuth titanate doped with V, Co and V+Co were investigated. Photochromic behavior was obtained. Holographic grating were recorded in all doped samples in visible range. Vanadium seems most promising dopand for future photorefrctive applications.

ACKNOWLEDGEMENTS

This work was supported by the contract 89-E-FA06-1-4 by the Ministry of Education, Taiwan, R.O.C. and Taiwan-Bulgarian collaboration program agreement NSC91-2911-I-009-010.

REFERENCES

1. A. Martin, D. Bravo, E. Dueguez, F. J. Lopez "Electron-paramagnetic resonance of thetrahedral Fe^{3+} in $Bi_4Ge_3O_{12}$ single crystals" Phys. Rev. B, **54**, 12915, 1996

2. P. A. Williams, A. H. Rose, K. S. Lee, D, C. Conrad, G.W. Day and P.D. Hale “Optical, thermo-optic, electro-optic and photoelastic properties of bismuth germanate” *Appl. Optics*, **35**, 3562-3569, 1996.
3. B. C. Grabmaier, "Crystal scintillators" *IEEE Trans. Nucl. Sci*. vol. **NS-31**, 372-376, 1984
4. R. Orlowski, E. Kratzig and H. Kurz, "Photorefractive effect in $LiNbO_3$:Fe under external electric field" *Opt. Comm*., **20**, 171-174, 1977.
5. G. Montemezzani, St. Pfandler and P. Gunter, "Electro-optic and photorefractive properties of $Bi_4Ge_3O_{12}$ crystals in the ultraviolet spectral range", *JOSA* B, **`9**, 1110-1117, 1992.
6. E. Moya, L. Contreras and C. Zaldo, " $Bi_4Ge_3O_{12}$:Cr: a new photorefractive materials" *JOSA* B, **5** (8), 1737-1742, 1988.
7. C. Zaldo and E. Dieguez, "On the microscopic origin of the photochromic and photorefractive behaviour of doped $Bi_4Ge_3O_{12}$ single crystals", *Opt. Mat*., **1**, 171-176, 1992.
8. C. Zaldo, E. Moya, F. Magana, L. Kovacs and K. Polgar, "Optically induced gratings in Fe- and Mn-doped $Bi_4Ge_3O_{12}$ single crystals", *J. Appl. Phys*., **73** (5), 2114-2121, 1993.
9. L. Kovacs, E. Moya, K. Polgar, F. J. Lopez and C. Zaldo "Photochromic behaviour of doped $Bi_4Ge_3O_{12}$ single crystals" *Appl. Phys. A*, **52**, 307-312, 1991.
10. K. Buse, A. Adibi and D. Psaltis “Non-volatile holographic storage in doubly doped lithium niobate crystals” *Nature*, **393**, 665-668, 1998.